Zeitschrift: Schweizerische mineralogische und petrographische Mitteilungen = Bulletin suisse de minéralogie et pétrographie

Band: 71 (1991)

Heft: 3

Artikel: Geochemistry and tectonic significance of Late Hercynian potassic and ultrapotassic magmatism in the Aar Massif (Central Alps)

Autor: Schaltegger, Urs / Gnos, Edwin / Küpfer, Theo

DOI: https://doi.org/10.5169/seals-54372

Nutzungsbedingungen

Die ETH-Bibliothek ist die Anbieterin der digitalisierten Zeitschriften auf E-Periodica. Sie besitzt keine Urheberrechte an den Zeitschriften und ist nicht verantwortlich für deren Inhalte. Die Rechte liegen in der Regel bei den Herausgebern beziehungsweise den externen Rechteinhabern. Das Veröffentlichen von Bildern in Print- und Online-Publikationen sowie auf Social Media-Kanälen oder Webseiten ist nur mit vorheriger Genehmigung der Rechteinhaber erlaubt. Mehr erfahren

Conditions d'utilisation

L'ETH Library est le fournisseur des revues numérisées. Elle ne détient aucun droit d'auteur sur les revues et n'est pas responsable de leur contenu. En règle générale, les droits sont détenus par les éditeurs ou les détenteurs de droits externes. La reproduction d'images dans des publications imprimées ou en ligne ainsi que sur des canaux de médias sociaux ou des sites web n'est autorisée qu'avec l'accord préalable des détenteurs des droits. En savoir plus

Terms of use

The ETH Library is the provider of the digitised journals. It does not own any copyrights to the journals and is not responsible for their content. The rights usually lie with the publishers or the external rights holders. Publishing images in print and online publications, as well as on social media channels or websites, is only permitted with the prior consent of the rights holders. Find out more

Download PDF: 19.07.2025

ETH-Bibliothek Zürich, E-Periodica, https://www.e-periodica.ch

SCHWEIZ. MINERAL. PETROGR. MITT. 71, 391–403, 1991

Geochemistry and tectonic significance of Late Hercynian potassic and ultrapotassic magmatism in the Aar Massif (Central Alps)

by *Urs Schaltegger*[1], *Edwin Gnos*[2], *Theo Küpfer*[3] and *Toni P. Labhart*[2]

Abstract

In the eastern Aar Massif (Central Alps, Switzerland) two different Upper Carboniferous intrusive series can be recognized: (A) A shoshonitic-ultrapotassic series, consisting of dioritic rocks of Val Punteglias, of the Giuv syenite and the Punteglias granite, and (B) a high-K calc-alkaline series consisting of the Düssi-Fruttstock diorite and the Brunni granite, both situated in the Brunnital. Both series originate from an enriched mantle source high in Rb, K and Th, but experienced different processes during their evolution. The shoshonitic-ultrapotassic series was possibly contaminated by partial melts of subducted slab sediments, but was hardly affected by fractionation processes; it therefore represents rather original material from the subcontinental mantle. The calc-alkaline series experienced extensive fractional crystallization and contamination by crustal melts.

The shoshonitic-ultrapotassic rocks were emplaced at a late stage of Hercynian orogeny. They were intruded after the cessation of compression and mark the beginning of late Hercynian strike-slip tectonics that enabled mantle melts to rise into the upper crust.

Keywords: ultrapotassic rocks, geochemistry, mantle-crust interaction, Hercynian magmatism, Aar Massif, Central Alps, Switzerland.

Introduction

Potassic and ultrapotassic rocks are rare but occur in various plate tectonic settings; they may be part of continental rift systems or intrude into regions of post-orogenic crustal extension and heating (e.g. THOMPSON et al., 1989). Shoshonitic to ultrapotassic rocks are widespread among ancient and modern volcanic and magmatic arcs, e.g. in the Eolian arc (ELLAM et al., 1989), Sunda-Banda arc (WHELLER et al., 1987), late tectonic plutons in the Grenville Province (CORRIVEAU, 1990) and also in Archean granite-greenstone terrains (SHIREY and HANSON, 1984). Shoshonitic to ultrapotassic rocks may also occur in orogenic settings, along active continental margins (THOMPSON and FOWLER, 1986).

Genetic models for shoshonitic-ultrapotassic rock associations often imply the existence of a LILE (large ion lithophile element)-enriched subcontinental mantle source; variable crustal contamination and different extents of fractional crystallization in intermediate and final magma chambers lead to a large geochemical diversity of different shoshonitic rock suites. The geotectonic setting is generally thought to be distant from the active subduction, thus the melts are of deep-seated mantle origin and were generated and fractionated in either hydrous or anhydrous environments.

We report here the occurrence of a potassic to ultrapotassic magmatic association of late Hercynian age, situated in the pre-Mesozoic basement of

[1] Centre de Géochimie de la Surface, CNRS, 1, rue Blessig, F-67084 Strasbourg, France.
[2] Mineralogisch-petrographisches Institut, Universität Bern, Baltzerstrasse 1, 3012 Bern, Switzerland.
[3] Nationale Gesellschaft für die Lagerung radioaktiver Abfälle (NAGRA), Parkstrasse 23, 5401 Baden, Switzerland.

the Central Alps. The aim of this paper is to describe the petrography, the geological setting and the geochemistry of these rocks and to summarize the current ideas about the genesis of these rocks as a basis for future work.

Geology

The Aar Massif is part of the pre-Mesozoic basement in the external zone of the Hercynian fold belt (Helvetic zone, FRISCH et al., 1990). The Helvetic nappes above the massif were removed during Alpine and post-Alpine uplift and erosion. The massif consists of Hercynian magmatic and volcanic rocks that were intruded into a polymetamorphic basement of pre-Hercynian age (Fig. 1). The late Hercynian intrusives contain granites, diorites, monzonites and syenites and were emplaced 334 to 298 Ma ago (SCHALTEGGER et al., 1991). Volcanic and volcaniclastic sequences occur throughout the whole massif (BÖHM, 1988; FRANKS, 1968 a, b; SCHENKER, 1986; MERCOLLI et al., 1988); field evidence and geochemical criteria are consistent with a similar Upper Carboniferous extrusion/deposition age for the volcanic rocks. The late Hercynian intrusive rocks can be subdivided into three different groups, according to geochemical signature and age:

(A) A shoshonitic to ultrapotassic suite (SUPS) in the eastern part of the massif, comprising the Giuv syenite (HUBER, 1948; LABHART and RYBACH, 1971; LABHART, 1977) and the diorites and granites of Val Punteglias (KÜPFER, 1977; SEEMANN, 1975), emplaced 334 Ma ago (SCHALTEGGER et al., 1991).

(B) A high-K calc-alkaline series (KCAS), comprising the diorite-granite complex of Brunnital (Düssi-Fruttstock diorite and Brunni granite; GNOS, 1988, SIGRIST, 1947) and various other dioritic to granodioritic rocks in the central part of the massif, altogether emplaced around 308–310 Ma (SCHALTEGGER et al., 1991).

(C) The highly differentiated Central Aar granite, the largest late Hercynian intrusion, was emplaced 298 Ma ago (SCHALTEGGER and VON QUADT, 1990; SCHALTEGGER et al., 1991). Its petrography and geochemistry is extensively described in SCHALTEGGER (1989, 1990) and thus will not be discussed in detail in this paper. Data of SCHALTEGGER (1990) are however included in some diagrams to allow direct comparison of all three magmatic stages.

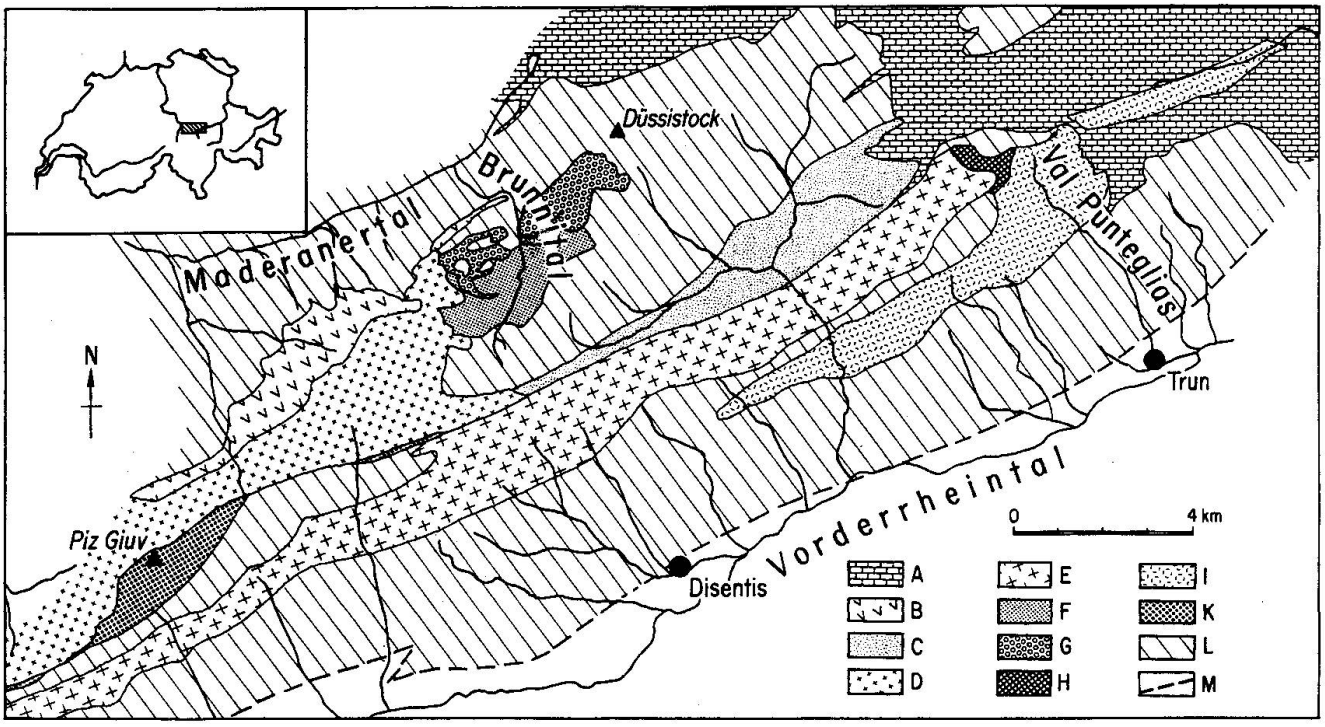

Fig. 1 Geologic sketch map of the central and eastern parts of the Aar Massif. Symbols: A) Sedimentary cover of the Aar Massif; B) Tscharren-Formation, volcaniclastic rocks; C) Val Gliems-Formation, volcaniclastic rocks; D) Central Aar granite; E) Southern Aar granite; F) Brunni granite; G) Düssi-Fruttstock diorite; H) Punteglias diorite; I) Punteglias granite; K) Giuv syenite; L) Polymetamorphic basement; M) Southern limit of the Aar Massif.

All rocks suffered a greenschist facies metamorphic overprint of Alpine age (FREY et al., 1980) that caused various mineral reactions and brittle to plastic deformation. This overprint modified geochemical compositions along shear zones (MARQUER, 1987) and disturbed or reset isotopic mineral systems (DEMPSTER, 1986). Late-Hercynian deformation and formation of mylonites must be envisaged, too.

Petrography of the investigated rocks

SHOSHONITIC-ULTRAPOTASSIC SERIES

This group includes three different rock units: The *diorites to monzodiorites of Val Punteglias* range from meladiorites and biotite-hornblendites to quartz-monzonites and quartz-monzodiorites in composition (Fig. 2). They consist of 8 to 10 small intrusive stocks, covering a total surface area of less than 1 km^2. The more mafic rock types are coarse-grained and contain up to 90% (by volume) of mafic minerals, the abundance of hornblende always exceeding biotite. The biotite-hornblende textures are considered to be magmatic. The mineral assemblage always contains normative ol. The more leucocratic quartz-monzonites and monzodiorites are fine-grained and inhomogeneous. On a mesoscopic scale, igneous layering is widespread in the monzosyenitic to dioritic rocks; the distribution of hornblende and biotite cumulates and plagioclase phenocrysts is patchy. The members of this group contain anhedral K-feldspar and euhedral acicular apatite, allanite, titanite, epidote, ilmenite, pyrite and zircon as accessory phases. The field relationships are typical for in-situ magma mixing: transitional contacts, layering with alternating crystal-rich horizons, magmatic flow textures and dioritic globules in a monzosyenitic matrix. Dykes crosscutting these rocks are generally more differentiated.

The *Punteglias granite* occurs in the same region, intruding into the diorites and suggesting a slightly younger age. It forms a lense-shaped body covering an area of 10 km^2 (Fig. 1). The granite ranges from a monzogranitic to granodioritic composition and can be subdivided in melanocratic, normal and leucocratic facies, respectively, and is rimmed and intruded by small stocks and dykes of a genetically related leucogranite, the Postabiala granite (SEEMANN, 1975). In the QAP diagram (Fig. 2) the granitic association reveals an increasing plagioclase/K-feldspar ratio in the very latest steps of differentiation. The granite contains large amounts of K-feldspar phenocrysts forming magmatic flow

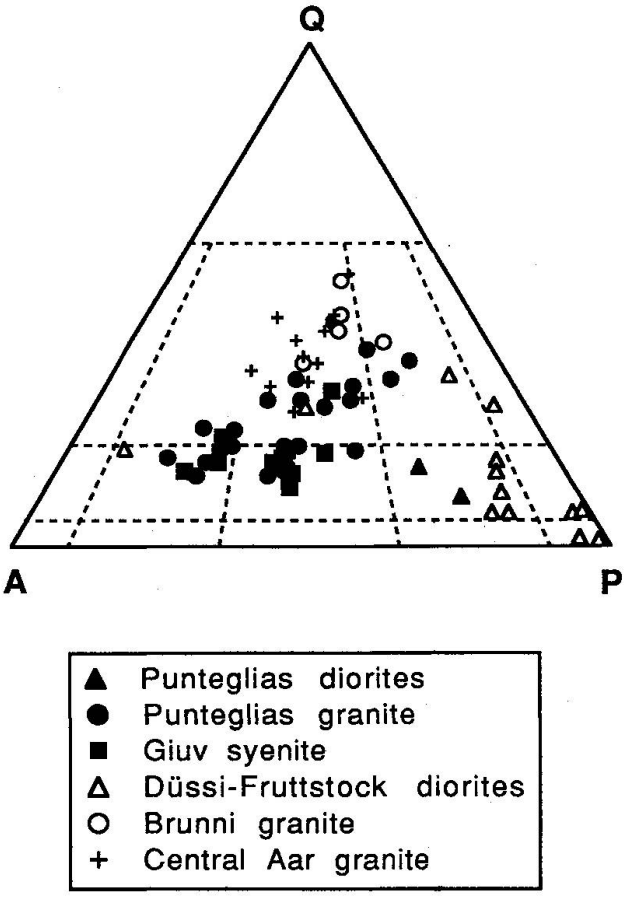

Fig. 2 QAP diagram showing the variation of modal compositions of the investigated rocks. Data from GNOS (1988), LABHART (1977), LABHART and RYBACH (1971), SEEMANN (1975); the two values for the Punteglias diorites are mean values of KÜPFER (1977) for a more mafic (meladiorite to biotite-hornblendite) and an intermediate group (quartz-monzonite to quartz-monzodiorite).

textures in a matrix of quartz, partly euhedral plagioclase (An 5–20), biotite and euhedral hornblende. Accessory minerals include apatite, titanite, epidote, allanite, zircon and opaques.

The *Giuv syenite* is the ultrapotassic member of this group; it occurs as a small lens (6 km^2) some 20 km west of Val Punteglias and has no visible connection with the above discussed rocks. It consists of a porphyritic coarse-grained central and a finer-grained marginal facies, both containing large euhedral K-feldspar phenocrysts showing magmatic flow textures. A second K-feldspar generation rims the phenocrysts and forms anhedral crystals in a matrix consisting of quartz, plagioclase and patches of biotite and hornblende. Accessories are titanite, apatite, zircon, allanite, epidote and opaques. Modal analyses plot in the fields of quartz-monzonite and quartz-syenite of a QAP diagram (Fig. 2). The normative mineralogy is partly SiO_2-undersaturated, few have normative ol.

HIGH-K CALC-ALKALINE SERIES

This group includes the leucocratic Brunni granite and an association of diorites in the region of Brunnital (Düssi-Fruttstock; Fig. 1). The *diorites* range from cumulate-like hornblende-gabbros to hornblende-diorites and hornblende- or biotite-quartz-monzonites. This wide range of intermediate rock composition can coexist at the scale of meters to decameters. The more mafic rock types typically occur as inclusions in more acid parts, sometimes forming magmatic breccia but more often having transitional contacts. These field characteristics suggest the contemporaneous intrusion of all rock types. Sometimes, they also contain angular xenoliths of biotite-plagioclase-gneiss or amphibolite from the adjacent basement. In more mafic rocks euhedral brown titanifereous hornblende cores are overgrown by green hornblende and titanite. Euhedral apatite and allanite/epidote occur as early liquidus phases, anhedral quartz, K-feldspar and plagioclase are late crystallizing phases. In some quartz-bearing rocks skeletal zircon was observed. Along the border of the intrusion, quartz-bearing diorites containing skeletal hornblende are common. Locally they are associated with pegmatoid pockets or dioritic globules in a syenitic matrix; towards the Brunni granite, K-feldspar phenocrysts are abundant.

The *Brunni granite* is a leucogranite containing 2–3 vol.% of mafic minerals. Large crystals of allanite/epidote are very characteristic. In a few places a border facies with K-feldspar megacrysts was observed. The granite is very homogeneous and shows a schistosity, presumably of Alpine age, which is more intense towards the south. An age of 308 ± 2 Ma was determined by SCHALTEGGER et al. (1991) from a diorite of this intrusive complex.

One sample of the *Schöllenen diorite* (Reuss valley, KAW 2520) has also been included in this study. This rock is coeval with the Düssi-Fruttstock diorite (SCHALTEGGER et al., 1991) and occurs as an enclave within the Central Aar granite.

Geochemistry

ANALYTICAL PROCEDURES

Geochemical analyses of the rocks from Val Punteglias are taken from KÜPFER (1977). Major and trace elements were analyzed by X-ray fluorescence (model Philips PW 1410) without specific matrix correction. Analytical precision is 50% concentration per weight ± 2% (relative), 1% ± 4%, 1000 ppm ± 6%, 50 ppm ± 15% (1 sigma standard deviations). K, Na, FeO, H_2O and CO_2 were determined using wet chemical methods.

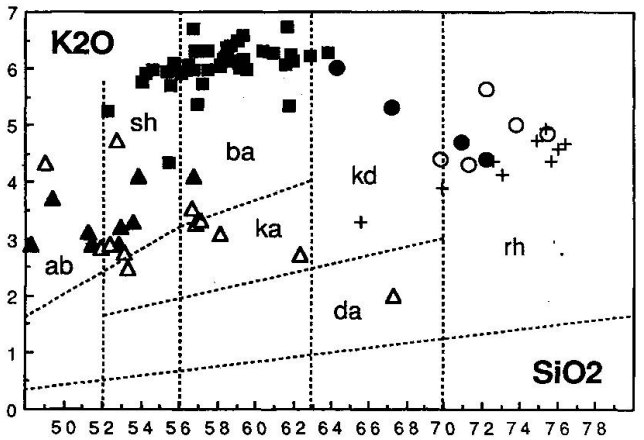

Fig. 3 K_2O vs SiO_2 (% per weight) diagram showing the classification of PECERILLO and TAYLOR (1976). Same symbols as in figure 2. The rocks of the shoshonitic-ultrapotassic suite (SUPS, filled symbols) lie in the fields of absarokite (ab), shoshonite (sh) and banakite (ba), the high-K, calc-alkaline rocks (KCAS) in the fields of absarokite, shoshonite, high-K andesite (ka) and dacite (da). Granites plot into the fields of high-K dacite (kd) and rhyolite (rh). The data for the Punteglias granite are mean values for different granite facies from SEEMANN (1975); Central Aar granite data from SCHALTEGGER (1989).

The geochemical data from the diorite-granite complex of the Brunnital are taken from GNOS (1988). Major elements were measured on fused rock tablets, trace elements on powder pills by XRF on a PW 1450 Philips spectrometer. Analytical errors are 50% ± 1%, 1% ± 5%, 1000 ppm ± 5%, 100 ppm ± 10%, 10 ppm ± 20% (1 sigma). FeO, H_2O and CO_2 were determined using wet chemical methods.

The Giuv syenite data were determined in 1989 at the Centre d'Analyse Minérale de l'Université de Lausanne on a Philips PW 1400 X-ray fluorescence spectrometer. Fused tablets were used for major elements, pressed powder pills for trace elements. Analytical errors are 50% ± 1%, 1000 ppm ± 5%, 100 ppm ± 10% (1 sigma). FeO, H_2O and CO_2 were determined using wet chemical methods.

The rare earth element analyses were carried out by Bondar-Clegg & Company Ltd. (Ottawa, Canada). Informations on analytical precision are not available. Detection limits are: La 0.5 ppm, Ce 5 ppm, Sm 0.1 ppm, Nd 10 ppm, Eu 1 ppm, Dy 1 ppm , Yb 0.5 ppm, Lu 0.1 ppm.

MAJOR AND TRACE ELEMENTS

The geochemical compositions for some representative samples are listed in table 1. The investigated rocks can be divided into two groups according to their geochemical characteristics:

Tab. 1 Major and trace element concentration of selected samples: Numbers 1 to 11 shoshonitic-ultrapotassic series (SUPS), 12 to 17 high-K, calc-alkaline series (KCAS). 1–4 Punteglias granite association (average values from SEEMANN, 1975): 1 melanocratic, 2 normal, 3 leucocratic facies, 4 Postabiala granite; 5–9 Giuv syenite: 5 coarse-grained (KAW 252), 6 enclave in the Central Aar granite (KAW 253), 7 and 8 both fine-grained (KAW 254 and 255), 9 coarse-grained (GS 23); 10–11 diorites Val Punteglias: 10 biotite-hornblendite (TK 196), 11 quartz-monzonite (TK 284), from KÜPFER (1977); 12–14 Düssi diorite: 12 hornblende diorite (EG 60), 13 biotite-hornblende diorite (EG 124), 14 biotite-hornblende tonalite (EG 126); 15–16 Brunni granite: leucogranites (EG 139 and 147), from GNOS (1988); 17 Schöllenen diorite: biotite-hornblende diorite (from SCHALTEGGER, 1989). Complete data set of the Giuf syenite analyses may be obtained on request from the first author.

	SUPS											KCAS					
	Punteglias granite				Giuv syenite					Punteglias diorite		Düssi diorite			Brunni granite		Schöllenen diorite
element	**1**	**2**	**3**	**4**	**5**	**6**	**7**	**8**	**9**	**10**	**11**	**12**	**13**	**14**	**15**	**16**	**17**
SiO2 (%)	64.2	67.2	70.9	72.2	58.69	58.57	62.86	61.85	47.32	48.3	53.6	53.31	49.04	58.14	69.82	75.41	59.10
TiO2	0.7	0.5	0.3	0.2	0.90	0.98	0.73	0.77	1.93	0.9	1.2	0.71	1.34	0.98	0.25	0.07	0.62
Al2O3	14.6	15.0	14.7	14.4	14.87	15.43	16.44	16.54	11.64	10.4	16.9	12.82	13.16	16.26	14.24	13.65	11.66
Fe2O3	0.8	0.6	0.7	0.4	4.97	5.34	3.95	4.21	2.49	1.6	1.6	1.84	1.18	1.51	0.74	0.44	6.22
FeO	3.0	2.1	1.1	1.2	n.d.	n.d.	n.d.	n.d.	n.d.	6.9	5.0	5.48	7.00	4.55	0.93	0.39	n.d.
MnO	n.d.	n.d.	n.d.	n.d.	0.08	0.09	0.07	0.08	0.18	0.2	0.2	0.16	0.20	0.13	0.05	b.d.l.	0.16
MgO	2.6	1.8	1.0	0.6	3.68	4.15	2.75	3.00	8.91	17.4	5.1	10.13	8.72	3.56	0.59	0.18	8.78
CaO	2.6	2.2	1.4	1.1	4.98	5.20	4.04	4.15	9.62	7.5	5.7	8.25	7.00	5.38	0.88	0.33	6.79
Na2O	3.1	3.3	3.9	4.2	2.64	2.72	3.17	3.29	0.74	1.2	3.5	3.18	3.57	3.97	5.04	3.73	2.77
K2O	6.0	5.3	4.7	4.4	6.14	6.24	6.21	6.26	5.13	2.9	3.3	2.48	4.33	3.07	4.42	4.86	3.23
P2O5	0.4	0.3	0.2	0.2	0.80	0.89	0.57	0.60	1.99	0.4	0.6	0.33	1.17	0.64	0.08	0.10	0.14
H2O	0.8	0.6	0.7	0.7	n.d.	n.d.	n.d.	n.d.	1.91	1.5	1.9	2.50	3.10	1.50	0.96	0.69	n.d.
Ba (ppm)	2275	2025	1475	1475	2649	2653	2311	2498	237	970	2250	1023	2324	1235	1184	355	1524
Rb	290	245	235	22	373	383	412	367	381	115	190	93	152	135	163	183	122
Sr	610	640	475	570	726	684	690	640	406	260	850	748	735	768	304	160	545
Pb	39	40	46	62	52	54	62	74	69	11	18	8	b.d.l.	7	22	28	36
Th	49	35	n.d.	37	79	80	105	108	46	n.d.	n.d.	20	15	12	5	2	31
U	10	11	n.d.	9	25	26	33	35	43	n.d.	n.d.	10	6	b.d.l.	b.d.l.	b.d.l.	18
Nb	n.d.	n.d.	n.d.	n.d.	25	25	29	35	33	n.d.	n.d.	15	34	19	6	9	30
La	n.d.	n.d.	n.d.	n.d.	68	71	35	71	39	n.d.	n.d.	31	185	106	42	4	52
Y	n.d.	n.d.	n.d.	n.d.	17	21	19	21	44	n.d.	n.d.	25	23	32	12	12	44
Zr	315	255	195	190	312	327	306	335	249	155	370	179	534	260	166	62	174
V	n.d.	n.d.	n.d.	n.d.	139	142	103	121	196	n.d.	n.d.	151	203	162	27	1	140
Zn	80	55	45	40	70	75	62	72	135	65	95	99	185	93	46	13	94
Sc	n.d.	n.d.	n.d.	n.d.	20	22	16	18	33	n.d.	n.d.	38	19	19	3	4	36
Cr	110	100	100	100	93	107	68	68	323	1200	105	505	360	97	3	b.d.l.	546
Ni	35	17	15	15	n.d.	n.d.	n.d.	n.d.	141	600	50	130	208	43	3	b.d.l.	n.d.
Co	12	10	10	10	n.d.	n.d.	n.d.	n.d.	44	74	29	38	39	27	13	7	n.d.
Cu	18	30	42	39	n.d.	n.d.	n.d.	n.d.	96	27	59	76	b.d.l.	b.d.l.	b.d.l.	b.d.l.	n.d.

abbreviations: n.d. = not determined; b.d.l. = below detection limit

(A) The shoshonitic-ultrapotassic series (SUPS) shows an increase in SiO_2 by 17%, in K_2O by 41% and a decrease in MgO by 71% from the most mafic to the most felsic samples. In the classification scheme of PECERILLO and TAYLOR (1976), which was established for volcanic rocks, most data points are situated in the absarokite, shoshonite and banakite fields, the granitic rocks plot into the high-K dacite and rhyolite fields (Fig. 3). The Giuv syenite is the only member that meets the requirements of the classification of FOLEY et al. (1987) for ultrapotassic rocks ($K_2O/Na_2O > 2\%$, $K_2O > 3\%$, $MgO > 3\%$).

The spidergram (chondrite-normalized variation diagram in order of increasing compatibility, THOMPSON, 1982; Fig. 4) of the SUPS reveals a LILE-enrichment in the Giuv syenite (samples KAW 252–255) and Punteglias granite (KAW 676), up to 3000 times chondritic values. An average diorite (major and trace elements: mean of 3 dioritic to monzodioritic samples from KÜPFER, 1977, REE of SU-89-10) and a biotite-hornblendite (TK 196) are considerably less enriched; the latter differs from the other rocks of the SUPS mainly by the smaller presence of Ba, Rb, Sr and LREE. Troughs at Nb (Ta), Sr and Ti are generally taken as indicators of a genesis by subduction-related processes (THOMPSON et al., 1984). For highly evolved rocks like the discussed syenites and granites, these troughs are astonishingly weak (see syenites of THOMPSON and FOWLER, 1986, for comparison). Compared to lamprophyres that are coeval with group C granites (OBERHÄNSLI, 1986) the SUPS rocks show stronger LILE-enrichment and less depleted Nb, P, Sr and Ti. According to their high Al_2O_3, CaO and relatively low MgO and TiO_2 contents, the ultrapotassic rocks are classified into group III of FOLEY et al. (1987), typical for orogenic ultrapotassic rocks. They, however, have higher LILE and lower contents on the more compatible end of the element selection (La to Yb) as well as less marked troughs for Nb, Sr and Ti, compared to group III standard rocks of FOLEY et al. (1987).

(B) The high-K calc-alkaline series (KCAS) starts with rocks of shoshonitic composition, too, but evolves towards lower potassium contents with increasing acidity (Fig. 3). It contains no ultrapotassic members. The leucogranitic counterpart, the Brunni granite, has K_2O contents around 5%, which are normal for high-Si melts. The spidergrams of the KCAS (Fig. 4) show a much smaller LILE-enrichment and are more irregular. The diorites exhibit large variations in La, Ce, Sr, P and Zr, whereas Nb and Ti are relatively consistent (Fig. 4), reflecting either variable allanite, plagioclase, apatite and zircon fractionation or mixing of melts with different compositions. Allanite certainly was an important fractionating mineral, judging from the highly variable Th, La and Ce concentrations. The Brunni leucogranite spidergram (Fig. 4) has more marked negative peaks at Ba, Th, Nb, P and Ti. The Ba depletion reflects K-feldspar crystallization in the latest stage of differentiation (MITTLEFEHLDT and MILLER, 1983; SCHALTEGGER and KRÄHENBÜHL, 1990).

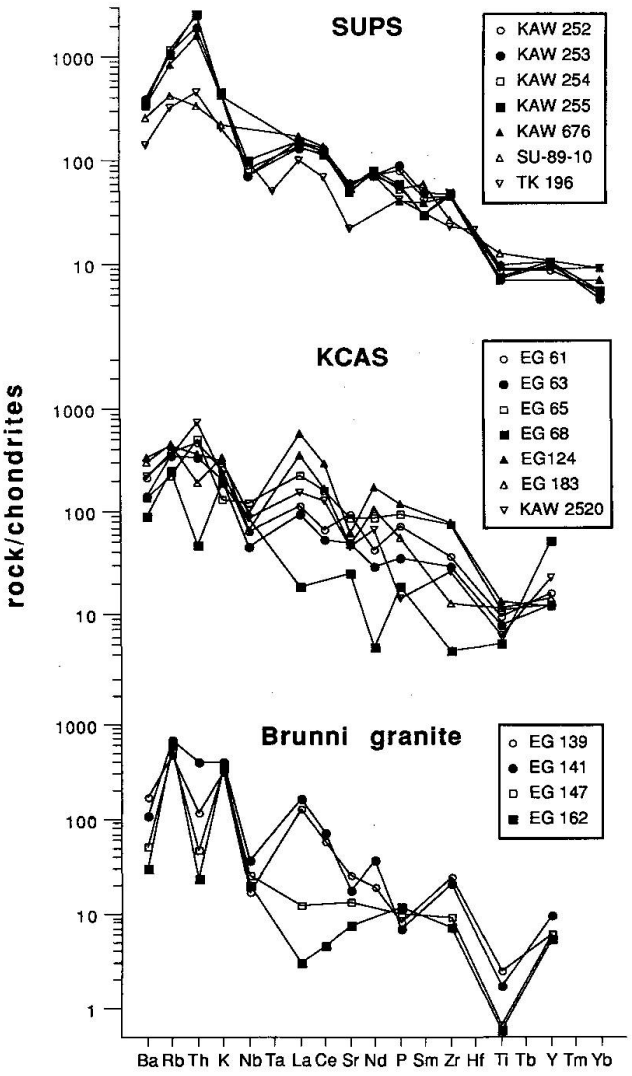

Fig. 4 Spidergrams (chondrite-normalized variation diagrams in increasing compatibility order, after THOMPSON, 1982; normalizing factors for Rb, K and P after SUN, 1980); shoshonitic-ultrapotassic series (SUPS): Giuv syenite (KAW 252–255), Punteglias granite (KAW 676) and diorites of Val Punteglias (SU-89-10, TK 196); high-K calc-alkaline series (KCAS): diorites of Düssi-Fruttstock complex (EG 61–183) and Schöllenen diorite (KAW 2520); and Brunni granite: leucogranites (EG 139, 141, 147, 162).

The Central Aar granite shows an evolution from the high-K dacite to rhyolite fields in the K_2O vs SiO_2 classification screen and thus follows a trend which is again different from the ones of the SUPS and KCAS.

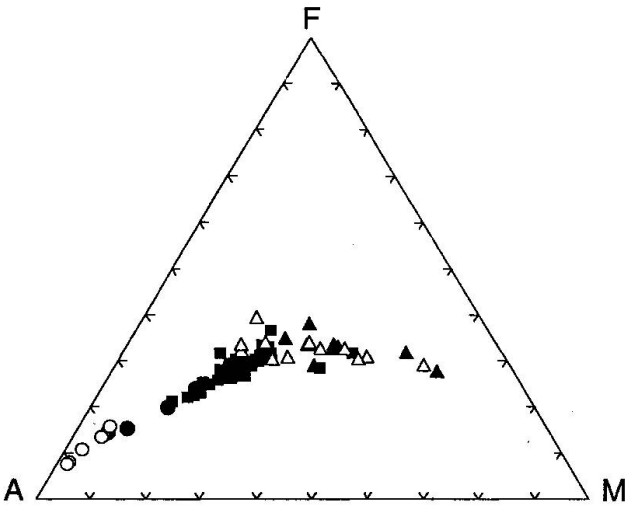

Fig. 5 AFM diagram. Same symbols as in figure 2.

The rocks of both SUPS and KCAS plot on a low-Fe calc-alkaline trend in a AFM diagram (Fig. 5) which is typical for shoshonitic series (MORRISON, 1980). The selected Harker diagrams (Fig. 6 a, b) show the compatible behaviour of Mg and Ti (similar relationship for P, Ca and Fe) and do not discriminate between the SUPS and KCAS. Smooth fractionation trends for higher silica rocks (Giuv syenite; Brunni, Punteglias and Central Aar

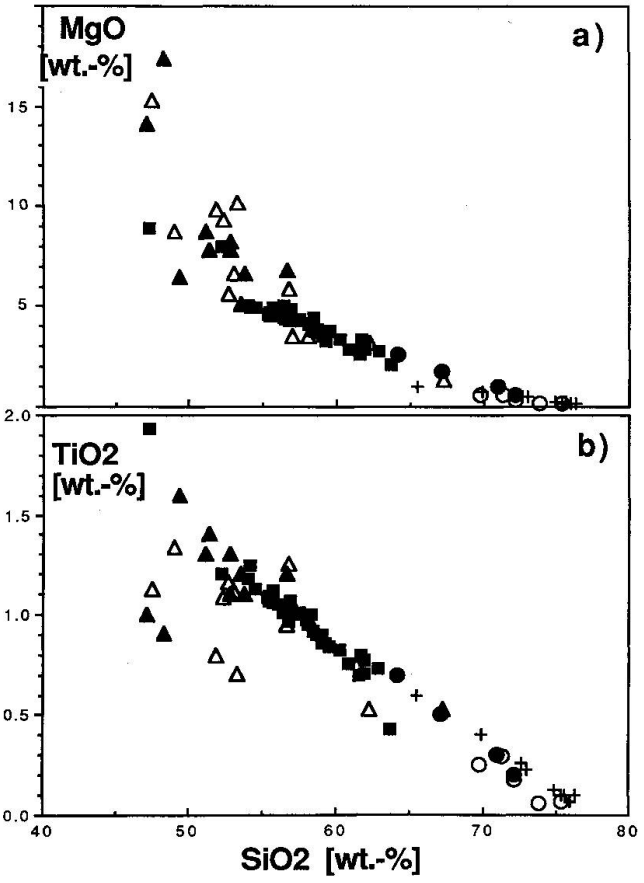

Fig. 6 Harker diagrams; a: MgO, b: TiO_2. Same symbols as in figure 2.

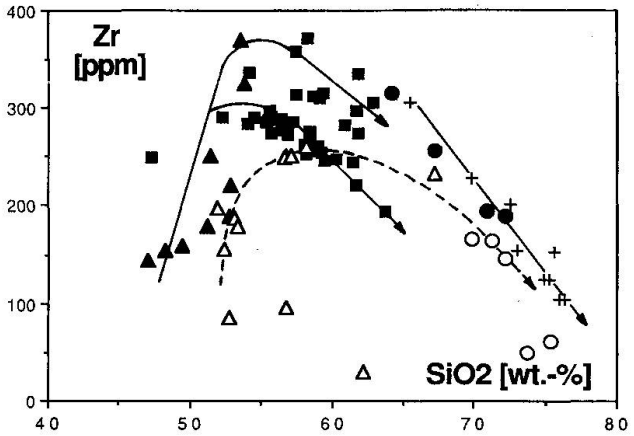

Fig. 7 Zr vs SiO_2 diagram. Same symbols as in figure 2.

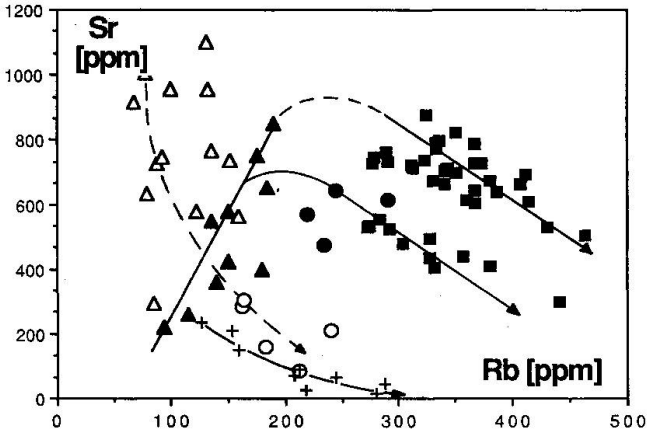

Fig. 8 Sr vs Rb diagram. Same symbols as in figure 2.

granites) contrast with the data scatter observed for the diorites, indicating the involvement of an additional process such as mixing of different melts or source components. K_2O, Na_2O, Th and U behave mostly incompatibly during the evolution of the SUPS, elements like Rb, Sr or Zr change to compatible geochemical behaviour at certain SiO_2 contents (Figs 7 and 8): Zr reaches saturation in the most silicic dioritic rocks; the syenite is saturated and shows a differentiation into two groups with higher and lower Zr contents, respectively (Fig. 7). The behaviour of Sr is similar: a low-Sr and high-Sr series can clearly be recognized (Fig. 8). They are not distinguishable on petrographical grounds and do not represent the separation into central and border facies at all. The Zr–SiO_2 systematic of the KCAS diorites is difficult to understand, but probably follows a similar evolutionary path as the SUPS diorites (Fig. 7); Rb and Sr, however, show a negative correlation (Fig. 8). Few outliers deviate from the trend lines in figures 7 and 8, which might be interpreted with mixing and/or cumulation processes.

The transition elements Mg, Cr and Ni are closely correlated for both series (Fig. 9 a, b), indi-

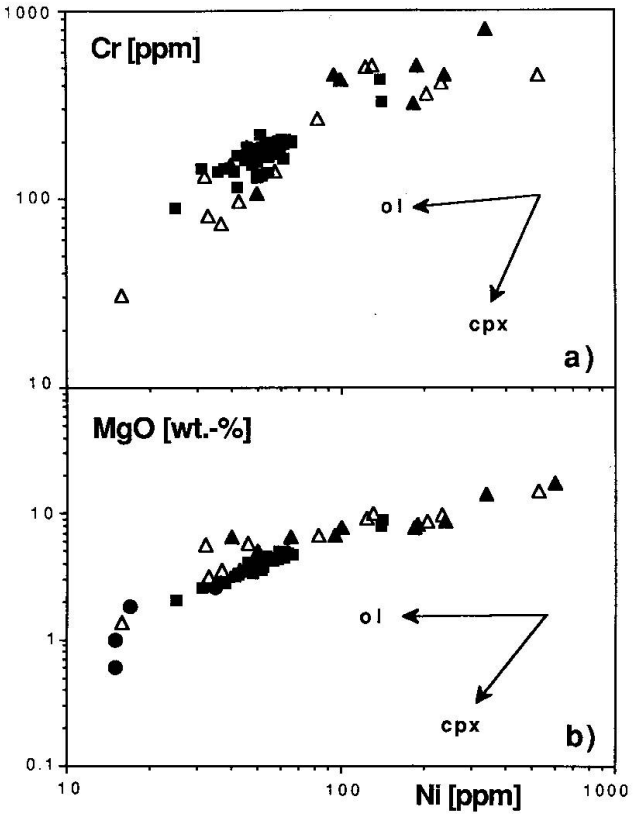

Fig. 9 *a:* Cr vs Ni; b: MgO vs Ni. Same symbols as in figure 2. Qualitative fractionation paths for olivine and clinopyroxene are indicated. Evolutionary trend shows a hiatus at 200 ppm Cr, 70 ppm Ni and 6% MgO, indicating a change from predominantly olivine to clinopyroxene-dominated fractionation at an early stage of magma evolution.

cating a two-stage evolution. It may be interpreted as a change in the ratio of olivine to pyroxene fractionation during the crystallization in a primary magma reservoir, or it may be created by another process than fractional crystallization (e.g. mixing), which would also explain the scatter of the dioritic rocks in figures 9 a and b.

RARE EARTH ELEMENTS

The rare earth element (REE) patterns of 8 samples, 6 from the SUPS and 2 from the KCAS, reveal a moderate enrichment of light rare earth elements (LREE; Fig. 10, Tab. 2). This feature is a characteristic of potassic rocks; similar or higher LREE contents can be found in modern ultrapotassic island arc volcanics (WHELLER et al., 1987). La_N/Yb_N values are highest in the Giuv syenite (24–28), lower in the Punteglias and Düssi diorites (18–20) and lowest in the Schöllenen diorite (9.6). There is little variation in the LREE concentrations; the differences are mainly caused by variable levels of heavy rare earth elements (HREE). A biotite-hornblendite from the SUPS (TK 196) has lower LREE concentrations suggesting lower bulk distribution coefficients for La to Sm, compared to the other samples.

The analyses do not show Eu anomalies despite the Sr variations in the spidergrams and high K-feldspar contents in the Giuv syenite. The lack of an Eu anomaly will be discussed in the next chapter. The patterns are similar to continental alkali basaltic trends (CHAUVEL and JAHN, 1984), but have lower LREE and higher La_N/Yb_N; they are smoother than patterns of the Aar Massif lamprophyres (OBERHÄNSLI et al., 1991), but show similar, slightly elevated HREE-plateaus.

Discussion

Both investigated rock suites consist mainly of dioritic and granitic rocks, intermediate syenites are only present in the SUPS and are lacking or undetected in the younger KCAS. The two series can be differentiated by means of their geochemical composition (Fig. 3). The shoshonitic-ultrapotassic series (SUPS), emplaced 334 Ma ago (SCHALTEGGER et al., 1991), is characterized by high LILE concentrations, elevated element ratios such as Ba/Sr, Ba/La, La/Yb, but low Rb/Sr and relatively primitive

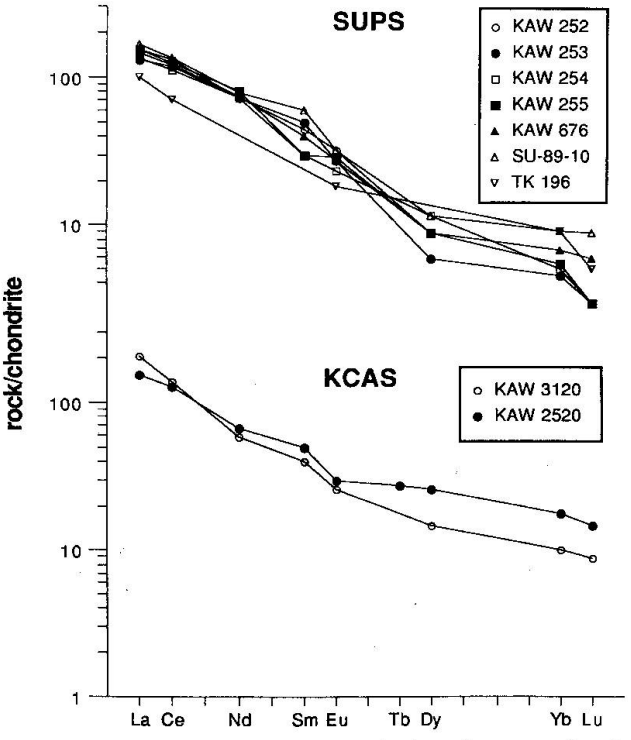

Fig. 10 Rare earth element variation diagrams for the shoshonitic-ultrapotassic series (SUPS) and two samples of the high-K calc-alkaline series (KCAS). For sample number identification see caption figure 4; KAW 3120 = biotite-hornblende diorite of Düssi-Fruttstock diorite complex. Normalizing factors of NAKAMURA (1974).

Tab. 2 Rare earth element concentrations. INAA determinations from Bondar-Clegg & Company Ltd., Ottawa, Canada.

sample	rock type	La [ppm]	Ce [ppm]	Nd [ppm]	Sm [ppm]	Eu [ppm]	Tb [ppm]	Dy [ppm]	Yb [ppm]	Lu [ppm]
KAW 252	Giuv syenite, c.g.	50	112	45	9	2.5	<1.0	3	1.2	0.1
KAW 253	Giuv syenite, f.g.	43	100	45	10	2.1	<1.0	2	1.0	0.1
KAW 254	Giuv syenite, f.g.	44	96	45	6	1.8	<1.0	4	1.1	0.1
KAW 255	Giuv syenite, c.g.	50	106	51	6	2.2	<1.0	3	1.2	0.1
KAW 676	Punteglias granite	48	105	47	8	2.1	<1.0	3	1.5	0.2
KAW 2520	Schöllenen diorite	50	109	42	10	2.3	1.3	9	3.9	0.5
KAW 3120	Düssi diorite	67	120	37	8	2.0	<1.0	5	2.2	0.3
SU-89-10	Punteglias monzo-diorite	55	117	49	12	2.5	<1.0	4	2.0	0.3

abbreviations: c.g. = coarse-grained, f.g. = fine-grained

REE patterns (Fig. 10). The rocks of the high-K calc-alkaline series (KCAS) are some 25 Ma younger (SCHALTEGGER et al., 1991) and show trace element patterns that are more typical of subduction-generated magmas, indicating a strong influence of fractionation processes. They also show primitive REE-patterns (Fig. 10), but no evident LILE anomaly.

The investigated rocks of both series are late orogenic intrusions and evolve to or occur together with contemporaneous or younger calc-alkaline granitoids (SCHALTEGGER and VON QUADT, 1990; SCHALTEGGER et al., 1991). Dioritic members of both series show clear field evidences for magma mixing, which is also indicated by a late K-feldspar crystallization in diorites and syenites. Abundant magmatic flow textures were generated during the emplacement of the phenocryst-containig melts in upper crustal levels, most spectacular for the K-feldspar-rich rocks (Giuv syenite and Punteglias granite). A weak post-emplacement deformation is present in all rock types and may be of late Hercynian and Alpine age.

THE ROLE OF FRACTIONAL CRYSTALLIZATION

The rocks of the SUPS show extensive liquidus crystallization (hornblende, biotite, titanite, apatite, allanite, zircon, plagioclase and K-feldspar) indicated by the presence of phenocrysts. During fractional crystallization, Rb, K_2O and especially Th must have behaved incompatibly, leading to anomalously high contents of U and Th in the Giuv syenite (mean values of 24 and 65 ppm, respectively; see also LABHART and RYBACH, 1971). This process, however, causes only weak fractionation troughs at La, Nb, Ti or Zr (Fig. 4) and no Eu-anomaly (Fig. 10) at all. The extent of the troughs in figure 4 does not change significantly from mafic to acid members of the SUPS, thus the low-pressure in-situ crystallization was not able to change these geochemical features. It must therefore be concluded that most of the geochemical characteristic is inherited from a common source. Any differentiation process as well as mixing with crustal components would, however, enhance the contents of Rb, Th and K. This may possibly contribute to the LILE-enrichment of the syenites of the SUPS (Fig. 4). Post-emplacement differentiation is indicated by systematic geochemical differences between different facies of the same rock type (core-rim of the Giuv syenite, see LABHART and RYBACH, 1971; melanocratic, normal and leucocratic facies of the Punteglias granite, see SEEMANN, 1975). Extensive fractional crystallization of minerals with K_D-values << 1 for LILE (pyroxenes, hornblendes, olivine) at an early magmatic stage would lead to considerable depletions in MgO, TiO_2, Cr or Ni, which is not the case for the SUPS rocks.

The rocks of the KCAS show evidence for fractional crystallization of biotite, hornblende, apatite, and eventually zircon, indicated by variable chondrite-normalized Sr, P, Ti and Zr concentrations in figure 4; largely variable La/Nb and Zr/Ti ratios may be caused by the removal of allanite and zircon. P and Ti peaks for KCAS and Brunni granite (Fig. 4) indicate that apatite fractionation is restricted to the dioritic stage and a subordinate process for the Brunni granite, whereas Ti depletion happened during the granitic stage, probably by fractionation of biotite and Ti-Fe-oxides. Compared to the SUPS fractional crystallization thus played a more important role in the genesis of the KCAS.

The importance of magma mixing processes is difficult to assess. In addition to field observations (GNOS, 1988; KÜPFER, 1977), mixing is indicated by

a large scatter in the geochemical data for the diorite samples of both series in some of the diagrams (Figs. 6 and 9). GNOS (1988) tentatively postulated a magma mixing process based on field evidence, but did not find a well fitting model.

SOURCE COMPOSITION

An assessment on compositions of parent melts remains very hypothetical without isotopic data. Compositions may be estimated from the most mafic and Mg-rich rocks of both suites. None of the investigated lithologies, however, strictly represents a pure melt composition; all of them contain phenocrysts of liquidus phases (allanite, apatite, hornblende/biotite, titanite, K-feldspar and plagioclase). The most mafic rocks of the SUPS have 14–17% MgO, 800–1200 ppm Cr and 300–600 ppm Ni; mafic analogues of the KCAS show contents of 10–15% MgO, 450–500 ppm Cr and 100–550 ppm Ni. Considering these concentrations, a genesis of both SUPS and KCAS rocks from a deep continental source can be ruled out.

The scattering data points of dioritic members of both SUPS and KCAS in figures 3, 6, 8 and 9 suggests a common or at least similar source composition for both series, more enriched in HREE and depleted in Nb, Sr, P and Ti for the KCAS. The hypothetical source is characterized by high LILE/LREE and LREE/HFSE (high field strength elements) ratios, as well as by high Th/U and low Rb/Sr ratios. It is more enriched in incompatible elements compared to ocean island or island arc volcanics (MORRISON, 1980; THOMPSON and FOWLER, 1986; THOMPSON et al., 1984).

There are three possible explanations for the LILE-enrichment: (A) a mantle source enriched in Ba, Rb, Th and K, (B) contamination of mantle melts by partial melts of a subducted slab and (C) contamination by crustal melts. The model of an enriched subcontinental mantle source is widely used to explain trace element patterns of subduction-related potassic to ultrapotassic rocks (FOLEY et al., 1987; STILLE et al., 1989; THOMPSON and FOWLER, 1986; WHELLER et al., 1987). Such a mantle source would have elevated Rb/Sr, Th/U, La/Nb ratios and LILE concentrations. The trace element characteristics and the similarity of the REE patterns from diorite to granite would also argue for the hypothesis of an enriched mantle source for the SUPS. A large numbers of different models for upper mantle enrichment have been suggested so far. STILLE et al. (1989) derive Hercynian lamprophyres from a metasomatically enriched mantle, which is, however, depleted in K_2O and enriched in Nb. Other models involve the rise of volatiles or melts into the upper mantle to produce magmas with primary hydrous mineral phases such as hornblende and mica (see FOLEY et al., 1987, for references). Such a model is consistent with the presented data set, because it allows the formation of high-K/Na ultrapotassic rocks by partial melting of a phlogopite-bearing peridotite. The high LILE concentrations as well as the elevated Ba/Sr ratios are the result of this enrichment process and therefore characteristic of the involved mantle source. The mantle enrichment by either volatiles or melts happened in connection with a subduction process of unknown age; it is a distinct process, separated by space and/or time, from contamination during the Hercynian subduction.

Partial melts of a subducted slab that contains pelagic sediments and oceanic crust can be highly enriched in incompatible elements (SCHREYER et al., 1987). Contamination with this material would lead to high Ba/La and Ba/Sr (STILLE et al., 1989). Ba/Sr ratios in the SUPS range from 2.4 up to 9.7, the crustal mean being around 0.9–1.1. Initial Sr ratios of the Giuv syenite range between 0.7073 and 0.7076 (unpublished data) and indicate either a volumetrically subordinate crustal contamination or contamination by melts from a low-Rb/Sr source. Considerable contamination by crustal melts (C) would cause much higher initial Sr ratios and low concentrations of Sr, Eu, Ti and P. The lack of a negative Eu anomaly as well as La_N/Yb_N ratios that are typical for alkali basalts, argue against this possibility. Crustal contamination is also indicated for the SUPS by low initial Hf isotopic compositions (SCHALTEGGER and CORFU, in prep.).

The rocks of the KCAS do not show the typical LILE-enrichment. The elemental variation in figure 4 may be interpreted as contamination of high-Cr, Ni, Ca, Sr mantle melts by crustal melts rich in Zr and LILE and low in Ba. The hybrid melts experienced fractional crystallization of titanite, ilmenite, zircon, apatite, plagioclase, pyroxenes and hornblende that caused scatter of Ti, Zr, Ca, P, Sr, Cr, Ni. The observed element scatter may consequently be the result of the combination of both processes. A mixing process is indicated in figure 11 (Ba/Sr vs Zr/Th diagram): a common source with Ba/Sr around 2.5 and a Zr/Th of 2 is mixed with crustal melts, causing a steep increase of the Zr/Th ratio and lowering the Ba/Sr ratio, and on the other hand with partial melts from the subducted slab, producing high Ba/Sr ratios (STILLE et al., 1989) and not changing the Zr/Th ratio. An alternative interpretation would be fractional crystallization: Assuming a bulk distribution coefficient $D_{Ba/Sr} > 1$, the Ba/Sr ratio might be enhanced by increasing modal content of K-feldspar, indicated by the data points of the Central Aar granite. The Zr/Th ratio

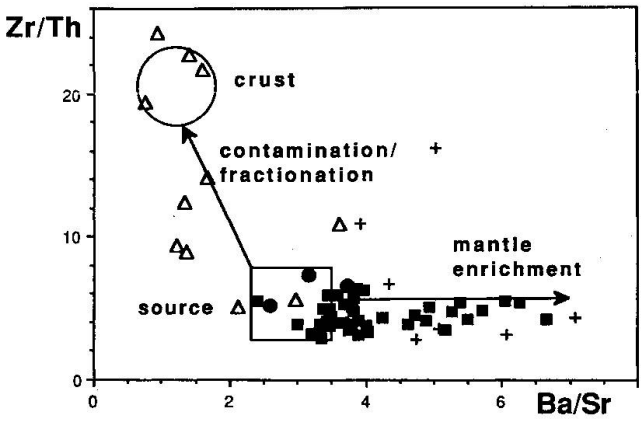

Fig. 11 Zr/Th vs Ba/Sr diagram. Same symbols as in figure 2. An original mantle source with Ba/Sr = 3 and Zr/Th = 4 was enriched during a subduction process involving sediments and leading to elevated Ba/Sr ratios of the shoshonitic-ultrapotassic rocks. The latter may be increased by K-feldspar accumulation. The high-K calc-alkaline rocks were possibly contaminated by crustal melts and experienced allanite fractionation, increasing the Zr/Th ratio in the melt.

on the other hand increases with the removal of allanite from the melt; such a process is indicated by highly variable La/Nb ratios in the KCAS (see Fig. 4). Figure 11 leads to the conclusion that different processes or mixing endmembers are responsible for the development of each of the two investigated rock series.

Tectonic implications

The results of the geochemical investigations indicate that the dioritic, syenitic, monzonitic and granitic rocks of the eastern Aar massif are derived from an enriched subcontinental mantle. The geochemical composition, the contamination by crustal melts or fluids and the occurrence in an orogenic setting certainly argues for a subduction-related genesis at some stage of the Laurasia-Gondwana collision. It is generally accepted that ultrapotassic magmatism may either be generated above active Andean-type subduction zones or as well in collisional belts, shortly after the closure of the ocean basin (THOMPSON et al., 1984; THOMPSON and FOWLER, 1986).

The nature and polarity of Hercynian subduction is still controversial, but most of the current models imply the presence of subducted oceanic crust (STILLE et al., 1989; MERCOLLI and OBERHÄNSLI, 1988). No preserved Paleozoic oceanic crust has been detected in the central Alpine segment of the Hercynides up to now, thus the complete consumption of the ocean basin must be envisaged. The obvious lack of a Hercynian high-grade high-T metamorphism or contemporaneous S-type magmatism favours the model of an Andean-type subduction zone rather than a classical continent-continent collision (FINGER and STEYRER, 1990). The active continental margin was formed by a magmatic arc that underwent considerable crustal shortening by upper crustal thin-skinned thrusting (OBERHÄNSLI et al., 1988) and possibly mid-crustal detachment faulting, as demonstrated by SHEFFELS (1990) for the Andes. The shoshonitic-ultrapotassic rocks are thought to be intruded into the thickened crust during a period of crustal relaxation or delamination.

The late Hercynian tectonic regime, creating strike-slip faults and pull-apart basins (BONIN, 1988; ZIEGLER, 1986), tapped the late-orogenic deep crustal magma chambers that generated large late Hercynian calc-alkaline batholiths in the Aar, Gotthard and Mont-Blanc massifs. The active continental margin had a more southern position at that time and the Andean-type subduction generated calc-alkaline magmas as young as Permian, e.g. the 262 Ma-old Lugano porphyries (STILLE and BULETTI, 1987). It is concluded that the onset of the slightly distensional, late Hercynian wrench tectonics is younger in the central region of the Hercynian fold belt than previously assumed, marked by the intrusion of the 334 Ma-old shoshonitic-ultrapotassic series of the Eastern Aar Massif.

Conclusions

Geochemical investigations on late Hercynian intrusive rocks of the Aar Massif lead to the following conclusions:

1. In the eastern Aar Massif, two different intrusive series exist that can be distinguished on geochemical basis: A shoshonitic-ultrapotassic suite, consisting of shoshonitic diorites, syenites and granites, is derived from an enriched mantle source; a high-K calc-alkaline series, consisting of shoshonitic diorites, monzodiorites and granites, is derived from the same or a similar source, but experienced extensive fractional crystallization and possibly contamination by crustal melts.

2. The subcontinental lithospheric mantle, which has been probed by the shoshonitic-ultrapotassic rocks, was geochemically enriched during a pre-Hercynian subduction event that created the characteristic geochemical features as LILE-enrichment and elevated Ba/Sr ratios, the latter due to the involvement of pelagic sediments.

3. The ultrapotassic rocks are typical of group III rocks of FOLEY et al. (1987) and have to be placed into an orogenic setting. Their generation

and emplacement is in direct relationship with an Upper Carboniferous Andean-type subduction.

4. The shoshonitic-ultrapotassic suite marks the beginning of late Hercynian strike-slip tectonics that created the pathways for the ascent of the voluminous late Hercynian magmatic rocks in the Aar Massif as well as in other parts of the Helvetic basement.

Acknowledgements

We wish to thank the staff of the Department of Mineralogy and Petrography in Bern, where the authors carried out their research, and of the departments in Fribourg and Lausanne, where parts of the analyses were performed. The paper was written during a fellowship of the Schweizerischer Nationalfonds to U.S. at the Royal Ontario Museum (Toronto, Canada), which is kindly acknowledged. The staff members of ROM Geochronology Lab are thanked for their help and hospitality. The manuscript benefitted of comments and fruitful discussions with F. Corfu and L. Heaman, both Toronto. The paper was reviewed by R. Oberhänsli, Mainz.

References

BÖHM, C. (1988): Vulkanoklastite im östlichen Aarmassiv (Val Russein, Graubünden). Schweiz. Mineral. Petrogr. Mitt. 68, 501–508.

BONIN, B. (1988): From orogenic to anorogenic environments: evidence from associated magmatic episodes. Schweiz. Mineral. Petrogr. Mitt. 68, 301–312.

CHAUVEL, C. and JAHN, B.-M. (1984): Nd–Sr isotope and REE geochemistry of alkali basalts from the Massif Central, France. Geochim. Cosmochim. Acta 48, 93–110.

CORRIVEAU, L. (1990): Proterozoic subduction and terrane amalgamation in the southwestern Grenville Province, Canada: Evidence from ultrapotassic to shoshonitic plutonism. Geology 15, 614–617.

DEMPSTER, T. (1986): Isotope systematics in minerals: biotite rejuvenation and exchange during Alpine metamorphism. Earth Planet. Sci. Lett. 78, 355–367.

ELLAM, R.M., HAWKESWORTH, C.J., MENZIES, M.A. and ROGERS, N.W. (1989): The volcanism of Southern Italy: Role of subduction and the relationship between potassic and sodic alkaline magmatism. J. Geophys. Res. 94, B4, 4589–4601.

FINGER, F. and STEYRER, H.P. (1990): I-type granitoids as indicators of a late Paleozoic convergent ocean-continent margin along the southern flank of the central European Variscan orogen. Geology 18, 1207–1210.

FOLEY, S.F., VENTURELLI, G., GREEN, D.H. and TOSCANI, L. (1987): The ultrapotassic rocks: Characteristics, classification and constraints for petrogenetic models. Earth-Sci. Rev. 24, 81–134.

FRANKS, G.D. (1968a): A study of upper Paleozoic sediments and volcanics in the northern part of the eastern Aar Massif. Eclogae geol. Helv. 61, 49–140.

FRANKS, G.D. (1968b): The pre-Westphalian (Hercynian) metamorphism and structures of the Tödi area (Aar Massif). Schweiz. Mineral. Petrogr. Mitt. 48, 667–694.

FREY, M., TEICHMÜLLER, M., TEICHMÜLLER, R., MULLIS, J., KÜNZI, B., BREITSCHMID, A., GRUNER, U. and SCHWIZER, B. (1980): Very low-grade metamorphism in external parts of the Central Alps: Illite crystallinity, coal rank and fluid inclusion data. Eclogae geol. Helv. 73, 173–203.

FRISCH, W., MÉNOT, R.-P., NEUBAUER, F. and VON RAUMER, J.F. (1990): Correlation and evolution of the Alpine basement. Schweiz. Mineral. Petrogr. Mitt. 70, 265–286.

GNOS, E. (1988): Geologie und Petrographie des westlichen Brunnitals (Maderanertal, Kanton Uri). Unpubl. diploma thesis, Univ. of Bern, 97 pp.

HUBER, W. (1948): Petrographisch-mineralogische Untersuchungen im südöstlichen Aarmassiv. Schweiz. Mineral. Petrogr. Mitt. 28, 555–642.

KÜPFER, Th. (1977): Mineralogisch-petrographische und geochemische Untersuchung der Syenodiorite und der Ganggesteine im Puntegliasgebiet (GR). Unpubl. Ph. D. thesis, Univ. of Bern.

LABHART, T.P. (1977): Aarmassiv und Gotthardmassiv. Sammlg. Geol. Führer 63, Borntraeger Berlin-Stuttgart, 173 pp.

LABHART, T.P. and RYBACH, L. (1971): Abundance and distribution of uranium and thorium in the syenite of Piz Giuf (Aar Massif, Switzerland). Chem. Geol. 7, 237–251.

MARQUER, D. (1987): Transfert de matière et déformation progressive des granitoïdes. Exemple des massifs de l'Aar et du Gothard (Alpes Centrales suisses). Mém. Docum. Centre Arm. Et. Struct. Socles, Rennes, 10, 287 pp.

MERCOLLI, I. and OBERHÄNSLI, R. (1988): Variscan tectonic evolution in the Central Alps: a working hypothesis. Schweiz. Mineral. Petrogr. Mitt. 68, 491–500.

MITTLEFEHLDT, D.W. and MILLER, C.F. (1983): Geochemistry of the Sweetwater Wash Pluton, California: Implications for "anomalous" trace element behaviour during differentiation of felsic magmas. Geochim. Cosmochim. Acta 47, 109–124.

MORRISON, G.W. (1980): Characteristics and tectonic setting of the shoshonite rock association. Lithos, 13, 97–108.

NAKAMURA, N. (1974): Determination of REE, Ba, Mg, Na and K in carbonaceous and ordinary chondrites. Geochim. Cosmochim. Acta 38, 757–775.

OBERHÄNSLI, R. (1986): Geochemistry of meta-lamprophyres from the Central Swiss Alps. Schweiz. Mineral. Petrogr. Mitt. 66, 315–342.

OBERHÄNSLI, R., SCHENKER, F. and MERCOLLI, I. (1988): Indications of Variscan nappe tectonics in the Aar Massif. Schweiz. Mineral. Petrogr. Mitt. 68, 509–520.

OBERHÄNSLI, R., KRÄHENBÜHL, U. and STILLE, P. (1991): Contrasting REE characteristics in meta-lamprophyres from Variscan Massifs of the Central Swiss Alps and REE patterns in lamprophyres from Variscan terranes of Western Europe. Schweiz. Mineral. Petrogr. Mitt. 71, 53–62.

PECERILLO, A. and TAYLOR, S.R. (1976): Geochemistry of Eocene calc-alkaline volcanic rocks from the Kastamonu area, Northern Turkey. Contrib. Mineral. Petrol. 58, 63–81.

SCHALTEGGER, U. (1989): Geochemische und isotopengeologische Untersuchungen am Zentralen Aaregranit und seinen assoziierten Gesteinen zwischen Aare und Reuss (Aarmassiv, Schweiz). Unpubl. Ph. D. thesis University of Bern, 144 pp.

SCHALTEGGER, U. (1990): The Central Aar Granite: Highly differentiated calc-alkaline magmatism in the Aar Massif (Central Alps, Switzerland). Eur. J. Mineral. 2, 254–259.

SCHALTEGGER, U. and CORFU, F.: An enriched subcontinental mantle source for late Hercynian magmatism in the Central Alps: Evidence from precise U–Pb ages and initial Hf isotopes (manuscript in preparation).

SCHALTEGGER, U. and KRÄHENBÜHL, U. (1990): Heavy rare earth enrichment in granites of the Aar Massif (Central Alps, Switzerland). Chem. Geol. 89, 1/2, 49–63.

SCHALTEGGER, U. and VON QUADT, A. (1990): U–Pb zircon dating of the Central Aar Granite (Aar Massif, Switzerland). Schweiz. Mineral. Petrogr. Mitt. 70, 361–371.

SCHALTEGGER, U., CORFU, F. and KROGH, T.E. (1991): Precise U–Pb ages and initial Hf isotopic compositions of late Hercynian mafic to acid intrusives in the Aar Massif, Central Alps. Terra abstracts 3, 37.

SCHENKER, F. (1986): Spätpaläozoischer saurer Vulkanismus und Beckenbildung im Aarmassiv unter kompressiver Tektonik. Unpubl. Ph. D. thesis, Univ. of Bern. 116 pp.

SCHREYER, W., MASSONNE, H.J. and CHOPIN, C. (1987): Continental crust subducted to depths near 100 km: implications for magma and fluid genesis in collision zones. In: MYSEN, B.O. (ed.), Magmatic Processes: Physicochemical Principles. Geochem Soc. Spec. Publ. 1, 155.

SEEMANN, U. (1975): Mineralogisch-petrographische und geochemische Untersuchungen der granitischen Gesteine der Val Punteglias (GR). Schweiz. Mineral. Petrogr. Mitt. 55, 257–306.

SHEFFELS, B.M. (1990): Lower bound on the amount of crustal shortening in the central Bolivian Andes. Geology 18, 812–815.

SHIREY, S.B. and HANSON, G.N. (1984): Mantle-derived Archean monzodiorites and trachyandesites. Nature, Nr. 310, 222–224, July 19, 1984.

SIGRIST, F. (1947): Beitrag zur Kenntnis der Petrographie und der alpinen Zerrkluftlagerstätten des östlichen Aarmassivs. Schweiz. Mineral. Petrogr. Mitt. 27, 39–183.

STILLE, P. (1988): Geochemische Aspekte der Krustenevolution im zentral- und südalpinen Raum. Habilitationsschrift ETH Zürich.

STILLE, P. and BULETTI, M. (1987): Nd–Sr isotopic characteristics of the Lugano volcanic rocks and constraints on the continental crust formation in the South Alpine domain (N-Italy-Switzerland). Contrib. Mineral. Petrol. 96, 140–150.

STILLE, P., OBERHÄNSLI, R. and WENGER-SCHENK, K. (1989): Hf–Nd and trace element constraints on the genesis of alkaline and calc-alkaline lamprophyres. Earth Planet. Sci. Lett. 96, 209–219.

SUN, S.-S. (1980): Lead isotope study of young volcanic rocks from mid-ocean ridges, ocean islands and island arcs. Phil. Trans. R. Soc. London, A 297, 409–445.

THOMPSON, R.N. (1982): Magmatism of the British Tertiary province. Scottish J. Geol. 18, 49–107.

THOMPSON, R.N. and FOWLER, M.B. (1986): Subduction-related shoshonitic and ultrapotassic magmatism: a study of Siluro-Ordovician syenites from the Scottish Caledonides. Contrib. Mineral. Petrol. 94, 507–522.

THOMPSON, R.N., MORRISON, M.A., HENDRY, G.L. and PARRY, S.J. (1984): An assessment of the relative roles of crust and mantle in magma genesis: an elemental approach. Phil. Trans. R. Soc. London, A 310, 549–590.

THOMPSON, R.N., LEAT, P.T., DICKIN, A.T., MORRISON, M.A., HENDRY, G.L. and GIBSON, S.A. (1989): Strongly potassic mafic magmas from lithospheric mantle sources during continental extension and heating: evidence from Miocene minettes of northwest Colorado, U.S.A. Earth Planet. Sci. Lett. 98, 139–153.

WHELLER, G.E., VARNE, R., FODEN, J.D. and ABBOTT, M.J. (1987): Geochemistry of quaternary volcanism in the Sunda-Banda Arc, Indonesia, and three-component genesis if island-arc basaltic magmas. J. Volcanol. Geotherm. Res. 32, 137–160.

ZIEGLER, P.A. (1986): Geodynamic model for the Paleozoic crustal consolidation of Western and Central Europe. Tectonophysics 126, 303–328.

Manuscript received March 1, 1991; revised manuscript accepted July 15, 1991.